Noise breakdown of landing aircraft using a microphone array and an airframe noise model

Simons, Dick; Snellen, Mirjam; Merino Martinez, Roberto; Malgoezar, Anwar

Publication date
2017

Document Version
Accepted author manuscript

Published in
Proceedings of the 46th International Congress and Exposition on Noise Control Engineering Taming Noise and Moving Quiet

Citation (APA)
Simons, D., Snellen, M., Merino Martinez, R., & Malgoezar, A. (2017). Noise breakdown of landing aircraft using a microphone array and an airframe noise model. In *Proceedings of the 46th International Congress and Exposition on Noise Control Engineering Taming Noise and Moving Quiet: Taming Noise and Moving Quiet, 27-30 Aug 2017 Hong Kong, China* (pp. 4361-4372)

Important note
To cite this publication, please use the final published version (if applicable).
Please check the document version above.

Noise breakdown of landing aircraft using a microphone array and an airframe noise model

Dick G. Simons; Mirjam Snellen; Roberto Merino-Martinez; Anwar M.N. Malgoezar

Section Aircraft Noise and Climate Effects

Faculty of Aerospace Engineering

Delft University Technology

2629 HS Delft

The Netherlands

ABSTRACT

For current generation aircraft, airframe noise is considered to have a significant contribution to the aircraft noise levels, especially during the landing phase. In this paper, a noise breakdown of landing aircraft is presented to investigate this airframe noise contribution. Use is made of data acquired with an acoustic array. The flyover measurements have been taken for a number of aircraft types in the landing phase. In addition, a model for predicting airframe noise is employed.

Conventional beamforming is applied for two frequency bands separately, i.e., 1500-4500 Hz and 4500-9500 Hz. From the resulting beamform source maps, and also from the spectrograms of the flyover data, engine noise is found to be clearly present in both frequency bands. Additionally, by comparing the measured overall sound pressure levels with the airframe noise model predictions, the engine noise is found to be dominant.

In agreement with the model predictions, the source plots reveal airframe noise to be present only in the lower frequency band. From the source plots it is found that there are clear differences between the different components (main landing gear, nose landing gear, flaps, slats) contributing to the airframe noise for the different aircraft types. These differences are partly in agreement with the model predictions, but discrepancies between model and data exist. Especially the nose landing gear is often clearly visible in the source plots, which is not expected from the model predictions. These differences can be considered to be a source of input to efforts for the further improvement of aircraft noise source models.

Keywords: aircraft flyover noise, microphone array measurements, beamforming, airframe noise modelling, model-data comparison, breakdown of aircraft noise sources I-INCE Classification of Subjects Number(s): T3.6

1. INTRODUCTION

Aircraft noise is a source of disturbance to the public, especially around airports. Apart from being annoying, noise pollution can also lead to health problems. With global air traffic growing at an average rate per year of about 5%, aircraft noise pollution is one of the main issues the aerospace industry is facing. Today aircraft noise levels are typically around 20 dB lower than they were 40 years ago, representing a significant reduction in the perceived noise level. However, over this period the number of air traffic movements has significantly increased, and will continue to grow [1]. Both technological and operational improvements are necessary to compensate for the impact of this growth.

To evaluate the noise impact on residents around airports, noise contours are determined, mostly based on model calculations. Hence, the corresponding noise regulations, with the purpose to balance aircraft operations and noise annoyance, are also based on these model calculations. These models provide noise levels given the distance, aircraft type and flight procedure. These predictions, which are partly based on information provided by aircraft manufacturers, e.g. gathered during certification, result in approximate and averaged values only [2], [3]. Moreover, earlier studies have shown that the observed noise levels for a certain fixed aircraft type, flight phase and location can vary considerably, even up to 12 dB [4]. In [5] it was shown that a measured variability of 8 dB is mainly due to the varying engine settings, in this case the fan rotational speed of the turbofan engines. Hence, it was concluded that it is necessary to incorporate engine setting into models for regulatory purposes around airports.

In the present research, noise assessment around an airport is performed experimentally by measuring noise from aircraft flyovers [5], [6], [7], [8], [9]. Such a study is obviously limited. We only study aircraft in the final landing phase (at a single location) with flaps and slats fully extended and landing gear deployed. However, a significant variety of aircraft types, ranging from small (Fokker 70) and medium size (Boeing 737, McDonnell Douglas 81, Airbus 321) to large (Boeing 747, Airbus 380) is considered.

The main sources of aircraft noise are the aircraft's engines and airframe (flaps, slats, landing gear). It is generally believed that airframe noise is important (sometimes even dominant), particularly during landing. The objective of this research is, therefore, to identify, for each of the six aircraft flyovers considered, the dominant noise sources and how this depends on aircraft type and frequency band. To this end, beamforming was applied using a small microphone array to a selection of the data from the aircraft flyovers described in detail in [10]. For each aircraft flyover considered, the measured power spectral density, i.e. the spectrum, is compared with predictions based on a semi-empirical airframe noise model with the purpose to determine the frequency bands where either engine noise is dominant or airframe noise contributes significantly. Subsequently, conventional beamforming [11] (in the frequency domain) is applied in these bands and the beamformed results at individual frequencies are incoherently added to suppress side lobes. From these resulting source plots the dominant noise sources for each landing aircraft can be deduced. The findings are of high importance for improving aircraft noise prediction models. Further, this paper can also be seen as complementary step compared to [5] where, as mentioned above, the aim was to identify causes of variability in the received aircraft noise.

The paper is organized as follows: Section 2 describes the experimental setup and the microphone array equipment. It also discusses the choice for the time snapshot (determining frequency resolution) and the spatial resolution of the microphone array. In addition, the aircraft geometrical data needed to run the airframe noise model is presented. Section 3 briefly presents the beamforming method applied. Also, the two frequency bands for incoherent processing are discussed and the effect of the chosen snapshot time on the resulting source plots is assessed. Section 4 presents the results. In section 4.1 the spectrograms of the entire flyovers are given, whereas section 4.2 presents the comparison of the spectrum predicted by the semi-empirical airframe noise model with that of the spectrum obtained for the 50 ms data when the aircraft is just above the microphone array. In section 4.2 more justification is given for the frequency bands of interest chosen. In section 4.3 a further model-data comparison is made, i.e., comparing the measured overall sound pressure level (OSPL) with that predicted by the airframe noise model. Section 4.4 presents the source plots for the six types of landing aircraft and the two frequency bands. From these plots the dominant noise sources for each landing aircraft can be deduced. Finally, section 5 contains the conclusions.

2. EXPERIMENTAL SETUP AND AIRCRAFT DATA

Flyover measurements were recorded at Amsterdam Airport Schiphol using a relatively small microphone array consisting of 32 microphones in a spiral distribution with an array aperture of 1.7 m, see figure 1 [12].

The microphone array was located 1,240 m to the South of the threshold of the Aalsmeerbaan runway, which is mainly used for landing. The microphone data are sampled at a frequency of 40 kHz. The data is band filtered in the frequency range from 45 Hz to 11,200 Hz. An optical camera was integrated in the centre of the array at a fixed angle facing straight up from the ground. The aircraft trajectories could be accurately estimated from this optical camera. The average flight height and average aircraft velocity were 67 m and 75 m/s, respectively, when the aircraft is directly above the microphone array. The exact height and velocity for each aircraft considered in this study is given in table 1. The meteorological data valid for the days of data acquisition can be found in [13]. For the analysis as presented in this paper a 50 ms snapshot is taken when the aircraft is exactly overhead. This corresponds to a frequency resolution of 20 Hz.

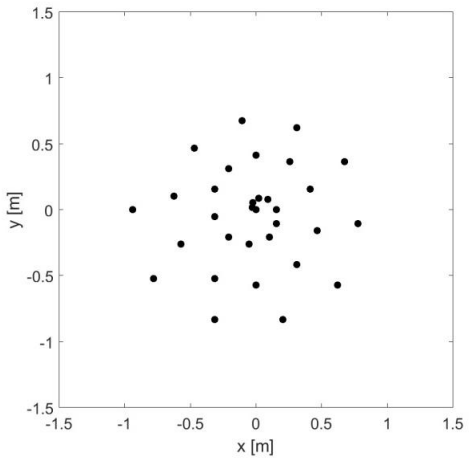

Figure 1: Microphone positions of the array used for the flyover measurements.

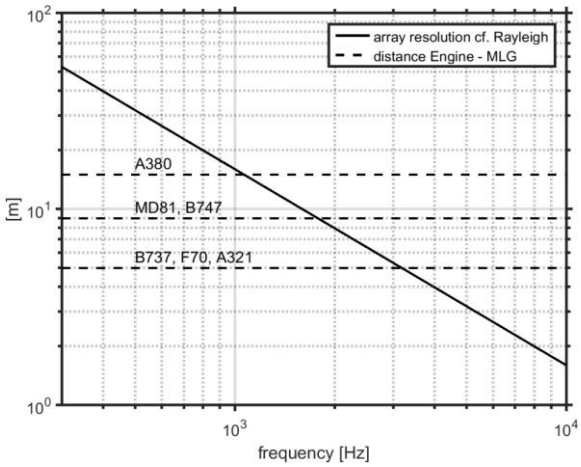

Figure 2: The array's spatial resolution as a function of frequency (solid line) calculated according to Rayleigh's criterion. For z_s we used 67 m, the average height of the aircraft considered. The horizontal dashed lines indicate the shortest distances between the engines and the main landing gear (MLG) for the six aircraft considered.

One of the objectives of this study is to separate airframe noise from engine noise. Specifically, it is interesting to see if we can separate the noise from the engines and the noise from the main landing gear. For sufficiently high frequency (i.e. larger than say 300 Hz), the array's theoretical spatial resolution according to Rayleigh's criterion (in m) is given by

$$\delta x = 1.22 \frac{z_s c}{Hf} \qquad (1)$$

with f frequency (in Hz), c sound speed (in m/s) and z_s the source (i.e. aircraft) height (in m). H is the aperture of the microphone array (1.7 m). δx is plotted as a function of f in figure 2. Also indicated (horizontal dashed lines) are the shortest distances between the engines and the main landing gear for the six aircraft considered. From the figure we may conclude that for the smaller aircraft (Boeing 737, Fokker70 and Airbus 321) resolving main landing gear from the engine noise is problematic as landing gear noise is expected to be only present at low frequencies (say below approximately 4 kHz). For the other aircraft we may expect to see the main landing gear noise to be separated from the engine noise in the beamform plots.

For the predictions of the airframe noise, use is made of the semi-empirical airframe noise model of Fink [14], [15]. This model requires input on flight parameters and the aircraft geometry. The aircraft height and speed, determined from the optical camera data (and confirmed by the available ADS-B and ground radar ATC data, see [10]), and the wing geometrical data, are given in table 1 below for all aircraft considered in this study. For the landing phase considered, both slats, flaps and landing gear are deployed. For the modelling we have assumed the flap angle to be 30° for all aircraft. In table 2 we have listed the landing gear data. The data listed in table 1 and 2 are used as input into the Fink model.

Table 1: Aircraft height, speed and wing geometrical data. [16], [17], [18], [19], [20], [21], [22]

Aircraft type	Height (m)	Speed (m/s)	Wing area (m^2)	Wing span (m)	Flap area (m^2)	Flap span (m)
Fokker 70	63.5	68	81	28	6.5	16
Airbus 321	64.5	75	98	34	10	22
MD 81	63.1	75	97	33	15	18
Boeing 737	70.4	81	130	34	18	17
Boeing 747	68.1	86	451	60	49	34
Airbus 380	64.9	72	753	80	103	42

Table 2: Aircraft landing gear data. [16], [17], [18], [19], [20], [21], [22]

	Main landing gear			Nose landing gear		
Aircraft type	Tire diameter (m)	Number of wheels/boggie	Number of boggies	Tire diameter (m)	Number of wheels/ boggie	Number of boggies
Fokker 70	1.1	2	2	0.7	2	1
Airbus 321	1.2	4	2	0.8	2	1
MD 81	1.1	2	2	0.7	2	1
Boeing 737	1.1	2	2	0.7	2	1
Boeing 747	1.2	4	4	1.2	2	1
Airbus 380	1.5	4	4	1.5	2	1

3. DESCRIPTION OF THE BEAMFORMING METHOD

We have applied conventional beamforming to the data in the frequency domain. The source plot or source map at frequency f_k is then given by

$$A(\boldsymbol{\xi}_j, f_k) = \frac{\mathbf{g}^*(\mathbf{P}\mathbf{P}^*)\mathbf{g}}{\|\mathbf{g}\|^2} \tag{2}$$

with * denoting the complex conjugate transpose. $\boldsymbol{\xi}_j$ is the position vector of grid point j in the defined scan plane. After Fourier transforming the acoustic time series data $p_m(t)$, the resulting Fourier coefficients $P_m(f_k)$ are put into the vector $\mathbf{P}$ (with index m referring to the microphone number). Vector $\mathbf{g}$ is the steering vector, the components of which are given as

$$g_m(\boldsymbol{\xi}_j, f_k) = \frac{\exp\left(-\frac{2\pi i f_k r_{m,j}}{c}\right)}{r_{m,j}} \tag{3}$$

$r_{m,j}$ is the distance from source position $\boldsymbol{\xi}_j$ to microphone m, whereas $r_{m,j}/c$ is the corresponding time delay ($i = \sqrt{-1}$). This steering vector implicitly assumes a monopole source model to describe the sound pressure field [8]. Also, the source is assumed to be non-moving, which is a valid approximation when the source is directly above the microphone array [23] (provided a small time interval is considered).

Beamforming is applied for a series of consecutive frequencies f_k within a certain band with a frequency step of 20 Hz as set by the snapshot time of 50 ms (see section 2).

For the conventional beamformer the spatial resolution at low frequencies is quite insufficient, whereas at high frequencies the source maps show many side and grating lobes. These two effects are counteracted by averaging the source plots calculated for the distinct frequencies f_k within the band according to

$$A_{\text{incoh}}(\boldsymbol{\xi}_j) = \frac{1}{N_f}\sum_{k=1}^{N_f} A(\boldsymbol{\xi}_j, f_k) \tag{4}$$

with N_f the number of frequencies in the band considered. This so-called incoherent averaging over frequencies averages away side and grating lobes that are differently positioned in the source plots at the various frequencies while at the same time preserving the good resolution at the higher frequencies.

The band-averaged source plots presented in section 4.4 have been obtained by taking the dB value of A_{incoh}, after correcting it for the aircraft distance z_s and after carefully calibrating vector $\mathbf{P}$.

Source plots are shown for two bands: 1500 – 4500 Hz and 4500 – 9500 Hz. In the lower frequency band airframe noise is expected to be important, whereas in the high-frequency band engine noise is expected to be dominant. The choice for these two frequency bands is further discussed in section 4.3, which presents a comparison of the measured spectrum to that calculated with the airframe noise model. The somewhat arbitrary lower bound of 1500 Hz is determined by spatial resolution considerations (below 1500 Hz the array's resolution becomes worse than 10 m, see figure 2).

Within the 50 ms snapshot the aircraft have moved by a distance of approximately 3.8 m, which is virtually equal to the resolution of the array at 4500 Hz, i.e. the frequency separating the two bands chosen. The array´s resolution in the middle of the low frequency band amounts to 5.4 m (see figure 2) , i.e., significantly larger than the distance flown by the aircraft. Hence, for the low-frequency band the 50 ms snapshot time is chosen short enough. For the high-frequency band, however, the movement of the aircraft may be visible to some extent in the source plots, since the resolution of the array in the mid of the high-frequency band (i.e. at 7000 Hz) is 2.3 m.

4. EXPERIMENTAL RESULTS

4.1 Spectrograms

In figure 3 the spectrogram for each aircraft flyover is shown. These spectrograms were calculated with a FFT size of 2048, corresponding to a time window (or time resolution) of 0.05 s. The corresponding frequency resolution in the spectrogram is then 20 Hz. For all aircraft, fan tones are clearly visible, indicating a strong engine noise contribution. Also, there is a significant contribution at high frequencies (> 4 kHz) where no airframe noise is expected. Whether engine noise is dominant or not can only be determined from the beamformed data, see section 4.4. Also the effect of the ground reflection, giving rise to an interference pattern, can be observed in most of the spectrograms.

For beamforming, a 50 ms snapshot of the data is selected close to the time at which the aircraft is directly above the microphone array, i.e. where the sound level is highest (and also the highest frequencies are observable in the spectrogram).

4.2 Model data comparison

This section presents a comparison of the spectrum measured for the 50 ms data (when the aircraft is just above the microphone array) with that predicted by the airframe noise model [14], [15],[24]. In figure 4 the power spectral density in dB/Hz is given as a function of frequency for the six aircraft considered. The calculated noise due to the wing, slats, flaps and main and nose landing gear are separately indicated. Also indicated is the total calculated power spectral density.

For all aircraft considered and for frequencies up to approximately 4500 Hz, the measured spectrum is only a few dB (less than 5 dB) higher than that calculated by the airframe noise model. From this it might be concluded that up to this frequency airframe noise is significantly contributing to the total noise of the aircraft. However, above 4500 Hz engine noise is dominant for all aircraft. This general observation justifies the two frequency bands chosen for beamforming, see section 3 and 5.4.

From the noise modelling of the individual airframe components also some specific observations can be made, see table 4. For the low frequency (LF) band chosen (1500 - 4500 Hz) this table gives the dominant airframe noise component for each aircraft type. For all aircraft noise from the clean wing and nose landing gear is negligible in this band. These aircraft type specific findings will be compared with the experimentally found dominant noise sources (see section 4.4).

Table 4: The dominant airframe noise component for each aircraft type according to the model in the LF band.

Aircraft type	Dominant airframe noise component
Fokker 70	Slats and flaps
Airbus 321	Main landing gear (and slats and flaps)
McDonnell Douglas 81	Slats and flaps
Boeing 737	Slats and flaps
Boeing 747	Main landing gear
Airbus 380	Main landing gear

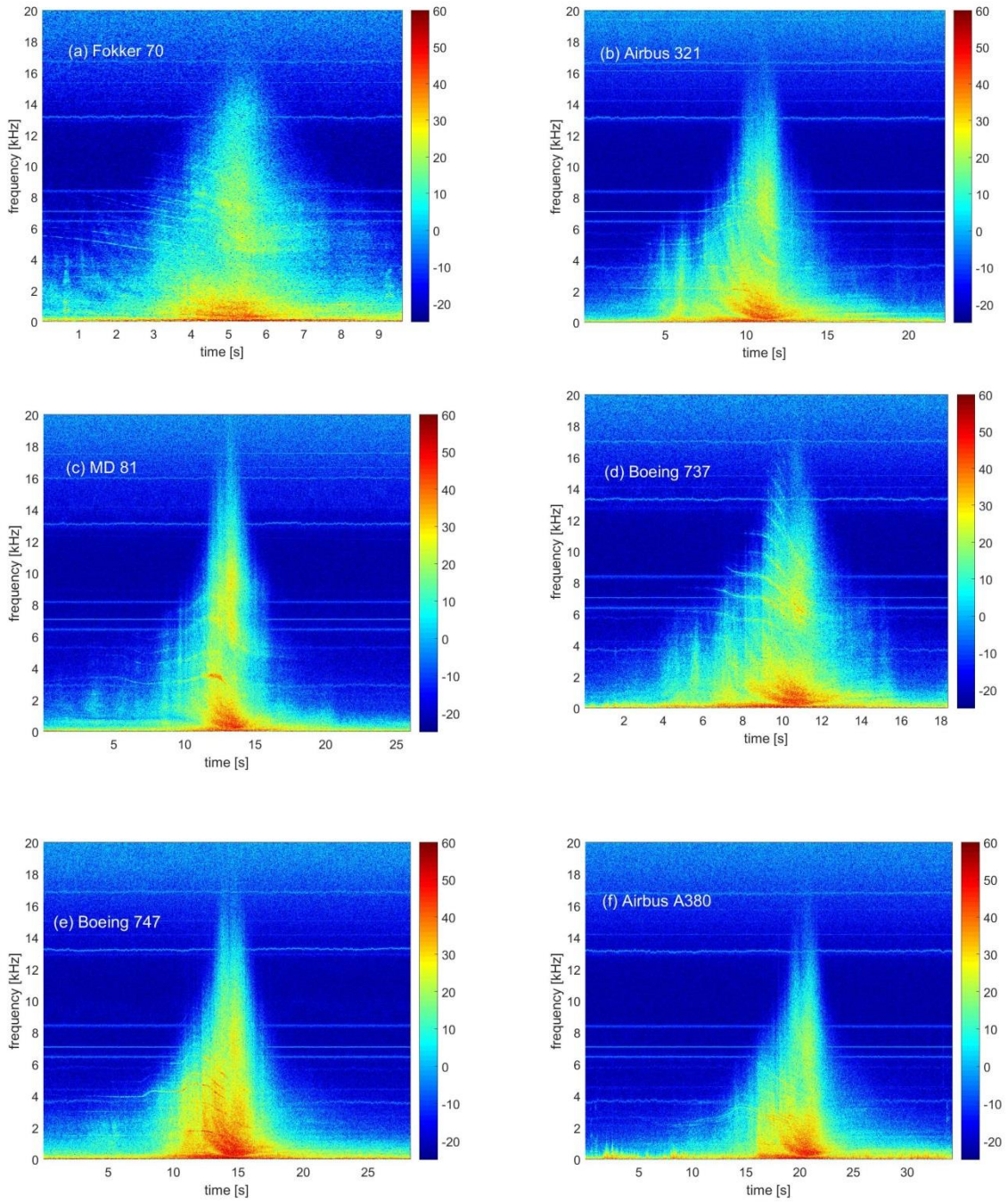

Figure 3: Measured spectrogram for each aircraft flyover considered.

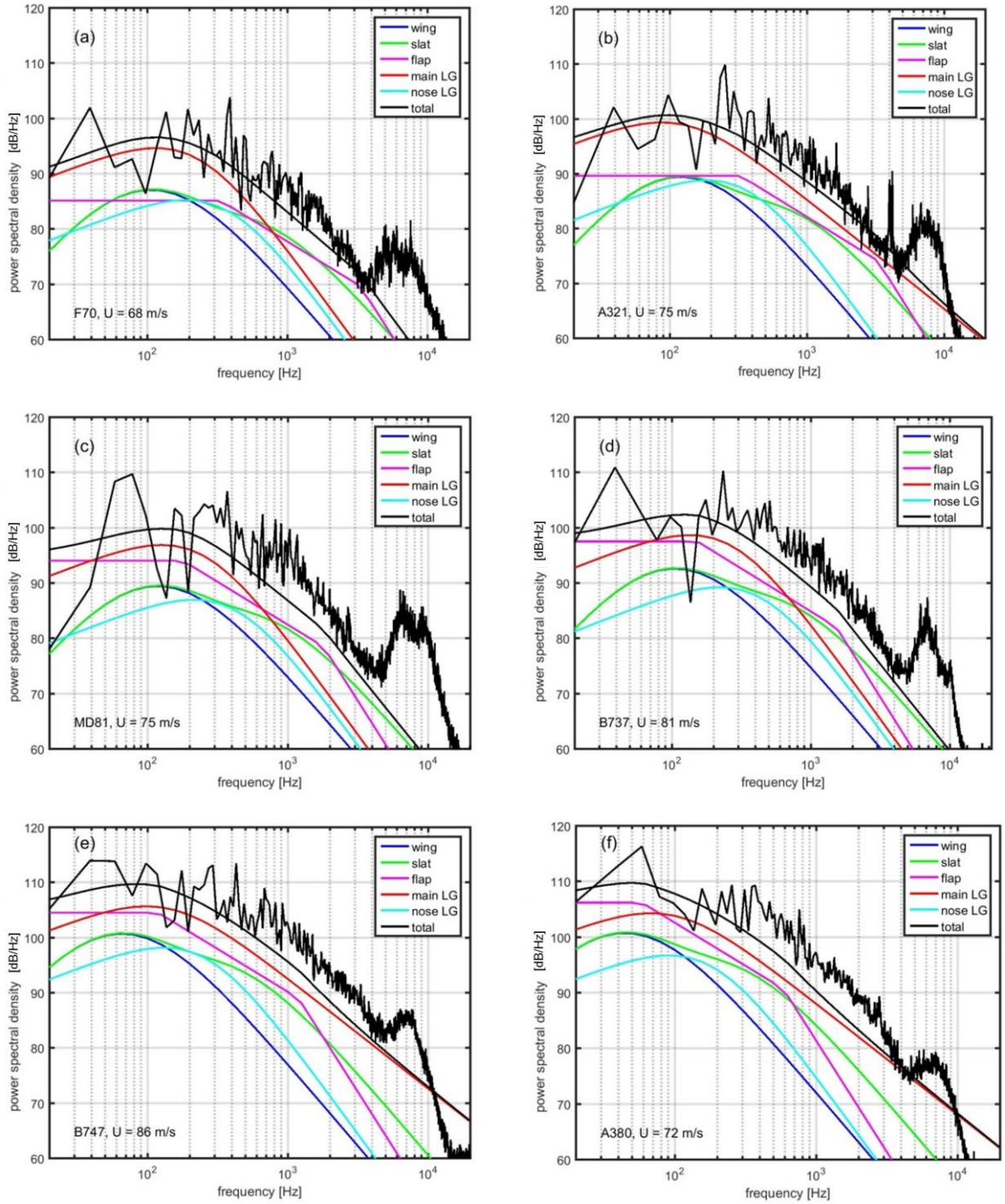

Figure 4: Measured spectrum compared to calculated spectrum for all six aircraft considered in this study. Both the modelled total power spectral density (smooth black line) as well as those calculated for the wing, slats, flaps and nose and main landing gear separately are indicated. Below approximately 100 Hz background noise might significantly contribute to the measured data. (a) Fokker 70 (b) Airbus 321 (c) McDonnell Douglas (d) Boeing 737 (e) Boeing 747 (f) Airbus A380.

4.3 Overall Sound Pressure Level (OSPL)

For each landing aircraft we determined the OSPL at overhead time according to

$$OSPL = 10 \log_{10} \left[\frac{\frac{1}{T} \int_0^T p^2(t)\, dt}{p_{ref}^2} \right] \tag{11}$$

with snapshot length T = 50 ms (see above), $p(t)$ the pressure time series (of one of the array's microphones) and $p_{ref} = 2\text{x}10^{-5}$ Pa. Subsequently, we corrected the obtained OSPL values for spherical spreading (adding $20 \log_{10}(z_s)$ dB), thereby getting the OSPL values at 1 m from the source. Atmospheric absorption is neglected. At the prevailing atmospheric conditions [10], [13] the absorption coefficients are $\alpha = 2\text{x}10^{-2}$ dB/m at 3000 Hz (center frequency of LF band) and $5\text{x}10^{-2}$ dB/m at 7000 Hz (center frequency of HF band). Hence, the absorption correction αz_s amounts to 1 dB and 3 dB at these frequencies, respectively. However, the contribution of high frequencies to the OSPL is about 20 dB less than that at the low frequencies, see figure 4. Neglecting absorption is thus resulting in an error considerably less than 1 dB.

In figure 5 we have plotted these measured OSPL values (averaged over all 32 microphones) against the OSPL values as obtained from the airframe noise model, including a least-squares fit line. Also indicated is the situation for which the experimental OSPL is entirely caused by airframe noise (dashed line), at least according to the model. Hence, we observe that for all landing aircraft considered here, engine noise is dominant by 4 to 5 dB.

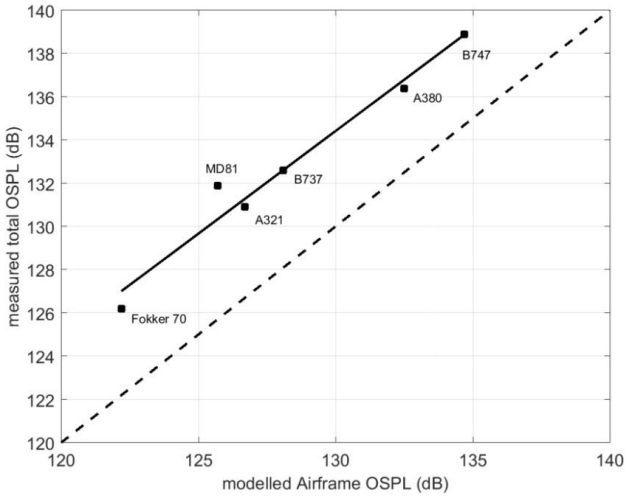

Figure 5: Measured Overall Sound Pressure Level (OSPL) plotted against the OSPL obtained from the airframe noise model for each aircraft type (squares). The solid line represents a least-squares fit through these data. The dashed line indicates the situation for which the experimental OSPL is entirely due to airframe noise. The solid line and dashed line are virtually parallel, indicating that engine noise is dominant by a fixed amount of 4-5 dB, independent of aircraft type.

4.4 Source plots

Using the broadband beamforming algorithm described in section 3 two source plots are presented for each landing aircraft considered in this study, i.e. a source plot for the band 1500 – 4500 Hz (denoted LF) and that for the band 4500 – 9500 Hz (denoted HF). The results, given in figures 6a and 6b, clearly show that aircraft noise sources, either the engines or airframe sources, can be identified. In each plot we have added the aircraft contour (black lines) on top of the beamform images, including the positions of the landing gear as indicated by the squares.

In all source plots, both for the LF and HF band, engine noise is present. However, for the LF band airframe noise sources are also clearly seen. An overview of the noise sources as observed in the source plots for each aircraft is given in table 5. It is interesting to compare these findings with the model predictions of table 4 in section 4.2. Indeed, some agreement between the measurements and

model outputs is observed. Further, the following specific observations are made for the LF band:

(1) Main landing gear noise is observed for the larger aircraft Boeing 747 and Airbus 380, which is confirmed by the airframe noise model; (2) Nose landing gear is often present in the data, especially for the smaller aircraft, although this is not predicted by the airframe noise model; (3) Flaps and slats are possibly observed for the Boeing 737 and for the McDonnell Douglas 81, which is confirmed by the model. However, the model also predicts flaps and slats to be dominant for the Fokker 70 and Airbus 321 and this is not seen in the measurements.

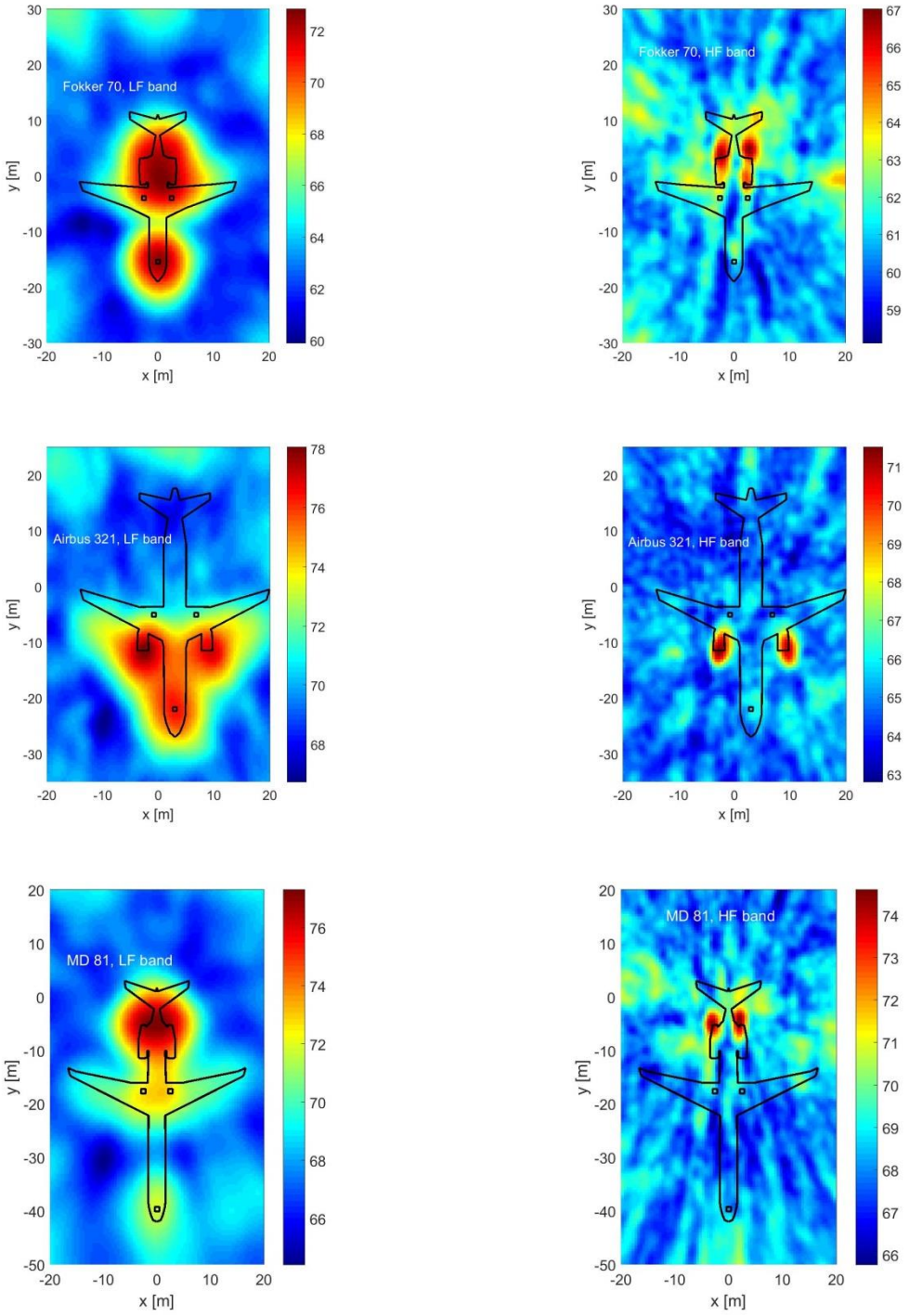

Figure 6a: Source plots for the LF band (left) and HF band (right) for the Fokker 70, Airbus 321 and McDonnell Douglas 81 flyover. The aircraft contour is indicated by a black line and the position of the main and nose landing gear is denoted by the black squares.

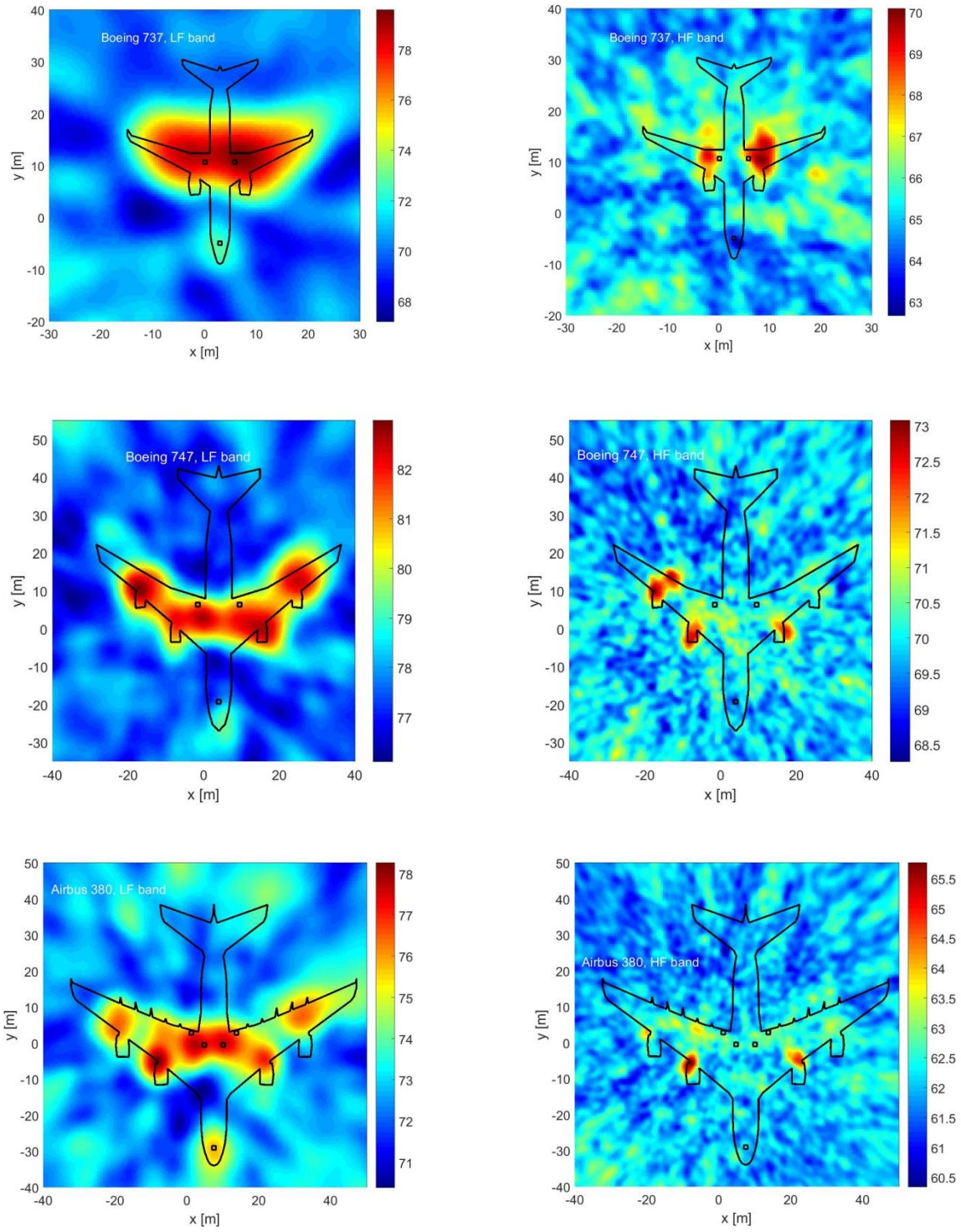

Figure 6b: Source plots for the LF band (left) and HF band (right) for the Boeing 737, Boeing 747 and Airbus 380 flyover. The aircraft contour is indicated by a black line and the position of the main and nose landing gear is denoted by the black squares.

Table 5: Dominant noise source in the source plots found for each aircraft. An ‘x’ denotes that a noise source is convincingly present, whereas (x) means ‘most probably present’. An ‘o’ indicates when an airframe noise source is dominant according to the model (see table 4).

aircraft	Engines (LF and HF)	Main LG (only LF)	Nose LG (only LF)	Flaps/slats (only LF)
Fokker 70	x		x	o
Airbus 321	x	o	x	o
McDonnell Douglas 81	x	x	x	(x)o
Boeing 737	x	(x)		(x)o
Boeing 747	x	xo		
Airbus 380	x	xo	x	

5. CONCLUSIONS

In this work an aircraft noise assessment was performed by measuring noise from aircraft flyovers at Schiphol airport. We have studied aircraft in the final landing phase with flaps and slats fully extended and landing gear deployed. Such an experimental study is necessarily limited. Still, a significant variety of aircraft types, ranging from small (Fokker 70) and medium size (Boeing 737, McDonnell Douglas 81, Airbus 321) to large (Boeing 747, Airbus 380) was considered.

The objective of this research is to identify, for each of the six aircraft flyovers considered, the dominant noise sources and how this depends on aircraft type and frequency band. To this end, conventional beamforming was applied to the aircraft noise data using a small microphone array. To suppress side lobes, the source plots obtained at individual frequencies were incoherently averaged over a band of frequencies. Source plots were calculated for two bands: 1500 - 4500 Hz and 4500 – 9500 Hz, denoted LF and HF band, respectively. The lower bound of the LF band was determined by spatial resolution considerations of the microphone array (i.e. worse than 10 m below 1500 Hz). These two frequency bands were basically determined from a comparison of the measured spectrum with predictions based on the semi-empirical airframe noise model of [14],[15]. From this comparison it was found that, for frequencies up to approximately 4500 Hz, the measured spectra are less than 5 dB higher than those calculated by the airframe noise model. This holds for all six aircraft flyovers and it was concluded that up to this frequency airframe noise is significantly contributing to the total noise of the aircraft. Above 4500 Hz engine noise is dominant for all aircraft.

In all source plots, both for the LF and HF band, engine noise is present. Actually, for the HF band only engine noise was seen, whereas for the LF band also airframe noise sources were clearly observed. Further, the following specific conclusions were made:

(1) Often airframe noise due to nose landing gear is observed experimentally (except for the Boeing aircraft), which is not sufficiently captured in the modelling; (2) Main landing gear noise is observed for the larger aircraft Boeing 747 and Airbus 380, which agrees well with the model predictions; (3) The model predicts flaps and slats to be an important noise source for the smaller aircraft, which is (to some extent) only confirmed experimentally for the McDonnell Douglas 81 and Boeing 737.

Finally, the measured overall sound pressure level (OSPL) as obtained from the pressure time series (and averaged over all 32 microphones) was compared with the OSPL values as obtained from the airframe noise model. From this it was observed that for all landing aircraft considered, engine noise is dominant by 4 to 5 dB. This engine noise dominance is in agreement with the observations made from the beamformed data.

The results presented in this contribution can also be seen as a step complementary to wind tunnel tests when the aim is to improve aircraft noise models. Wind tunnel measurements allow for controlled conditions, but are limited in their capability to represent operational conditions. The measurements described here are carried out under less controlled conditions, but do reflect these operational circumstances. When improving aircraft noise models, we believe that both approaches are needed.

REFERENCES

1. Boeing Commercial Airplanes. Current Market Outlook 2013-2032. USA 2013.
2. Zubrow, A., Hwang, S., Ahearn, M., Hansen, A., Koopmann, J., Solma, G., "Aviation Environmental Design Tool (AEDT), Version 2c, User Guide", U.S. Department of Transportation, Federal Aviation Administration, Report number DOT-VNTSC-FAA-16-16, 12 September 2016.
3. Ahearn, M., Boeker, E., Gorshkov, S., Hansen, A., Hwang, S., Koopmann, J., Malwitz, A., Noel, G., Reherman, C., Senzig, D., Solma, G., Tosa, Y., Wilson, A., Zubrow, A., DiPardo, J., Majeed, M., Bernal, J., Biederman, A., Dinges, E., Rickel, D., Yaworski, M., Hall, C., Augustine, S., Foley, R., "Aviation Environmental Design Tool (AEDT), Technical Manal, Version 2c", U.S. Department of Transportation, Federal Aviation Administration, Report number DOT-VNTSC-FAA-16-17, 12 September 2016.
4. Bergmans, D., Arntzen, M., and Lammen, W., "Noise Attenuation Directly Under the Flight Path," National Aerospace Laboratory/NLR, Rept. NLR-TP-2011-262, Amsterdam, 2011.
5. Simons, D. G., Snellen, M., Midden, B., Arntzen, M. and Bergmans D. H. T., "Assessment of noise level variations of aircraft fly-overs using acoustic arrays," Journal of Aircraft, Vol. 52, No. 5, pp 1625-1633, September-October 2015.
6. Michel, U., Barsikow, B., Helbig, J., Hellmig, M., Schüttpelz, M., "Flyover noise measurements on landing aircraft with a microphone array", AIAA Paper 98-2336, 4th AIAA/CEAS Aeroacoustics Conference, Toulouse, France, June 2-4, 1998.
7. Sijtsma, P., van der Wal, H.M.M., "Identification of noise sources on civil aircraft in approach using a phased array of microphones", Report No. NLR-TP-2004-166, National Aerospace Laboratory NLR, 2004.
8. Sijtsma, P., "Phased array beamforming applied to wind tunnel and fly-over tests", Report No. NLR-TP-2010-549, National Aerospace Laboratory NLR, 2010.
9. Siller, H.A., "Localisation of sound sources on aircraft in flight", BeBeC-2012-01, Berlin Beamforming Conference, Berlin, Germany, 22-23 February, 2012.
10. Merino-Martinez, R., Snellen, M. and Simons D.G., "Functional beamforming applied to imaging of fly-over noise on landing aircraft", accepted for the Journal of Aircraft, 2016.
11. Mueller, T. J. (Ed.), Aeroacoustic Measurements. First edition 2002. Springer-Verlag Berlin Heidelberg. ISBN-978-3-642-07514-8.
12. Rick van der Goot, Jorg Hendriks, Kirk Scheper, Giel Hermans, Wouter van der Wal and Dick G. Simons, "A low cost, high resolution acoustic camera with a flexible microphone configuration", 4th Berlin Beamforming Conference, 22-23 February 2012.
13. Snellen, M., Merino-Martinez, R. and Simons, D.G., "Assessment of noise level variability on landing aircraft using a microphone array", submitted for publication in the Journal of Aircraft, 2016.
14. M.R. Fink, "Noise component method for airframe noise", AIAA 4th Aero-acoustic conference, October 3-5, Atlanta, Georgia, USA, number AIAA 1977-1271, 1977.
15. M.R. Fink, "Airframe noise prediction method", FAA-RD-77-29, 1977.
16. Fokker 70/100 - Civil Aircraft Forecast International. 2002.
17. Fokker 70 Airplane characteristics - Pavement data. Landing gear footprint. 1995.
18. Airbus A320 - Aircraft characteristics airport and maintenance planning. Blagnac, France. 2005.
19. McDonnell Douglas MD-80 Series - Airplane characteristics for airport planning. Long Beach, USA. 1990.
20. Boeing 737 - Airplane characteristics for airport planning. Boeing commercial airplanes, USA 2013.
21. Boeing 747-400 - Airplane characteristics for airport planning. Boeing commercial airplanes, USA 2002.
22. Airbus A380 - Aircraft characteristics airport and maintenance planning. Blagnac, France. 2005.
23. Barsikow, B., King, W.F., "On removing the Doppler frequency shift from array measurements of railway noise", Journal of Sound and Vibration, 120 (1), pp. 190-196, 1988.
24. W.E. Zorumski, "Aircraft noise prediction program theoretical manual", NASA TM 83199, 1982.